

Evaluation of Electrochemiluminescent Metabolic Toxicity Screening Arrays Using a Multiple Compound Set

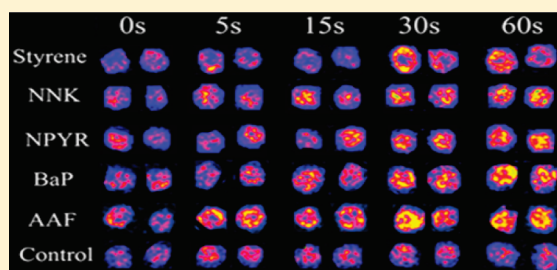
Shenmin Pan,[†] Linlin Zhao,[†] John B. Schenkman,[§] and James F. Rusling^{*,†,‡,§}

[†]Department of Chemistry and [‡]Institute of Materials Science, University of Connecticut, Storrs, Connecticut 06269, United States

[§]Department of Cell Biology, University of Connecticut Health Center, Farmington, Connecticut 06032, United States

S Supporting Information

ABSTRACT: Arrays for screening metabolite-generated toxicity utilizing spots containing DNA, enzyme, and electroluminescent (ECL) polymer ($[\text{Ru}(\text{bpy})_2\text{PVP}_{10}]^{2+}$) were extended to include a fully representative set of metabolic enzymes from human and rat liver microsomes, human and rat liver cytosol, and mouse liver S9 fractions. Array use involves two steps: (1) enzyme activation of the test chemical and metabolite reaction with DNA, and then, (2) capture of ECL resulting from DNA damage using a charge coupled device (CCD) camera. Plots of ECL increase vs enzyme reaction time monitor relative rates of DNA damage and were converted into turnover rates for enzymic production of DNA-reactive metabolites. ECL turnover rates were defined by R , the initial slope of ECL increase versus enzyme reaction time normalized for amounts of enzyme and test chemical. R -values were used to establish correlations for 11 toxic compounds with the standard toxicity metrics rodent liver TD_{50} and lethal dose (LD_{50}), Ames tests, and Comet assays for in vitro DNA damage. Results support the value of the ECL genotoxicity arrays together with toxicity bioassays for early screening of new chemicals and drug candidates.



Reactive metabolites of foreign chemicals can react with DNA bases to form covalent adducts that are good biomarkers for toxicity exposure.^{1–3} Consequently, detecting reactions of metabolites with DNA is an effective approach for safety assessment of new chemicals and drugs.^{4,5} DNA damage resulting from parent compounds or reactive metabolites is often referred to as genotoxicity. Species reacting with DNA may also react with proteins and other biomolecules.⁶

In vitro bioassays are used extensively in the pharmaceutical industry to help predict human toxicity.^{4,5,7} Toxicity bioassays are generally combined into a panel that provides a reasonably good prediction of human toxicity.⁷ However, behavior of a given chemical in specific individuals with unique biochemistry is difficult to predict from assay panel results. Animal testing is widely used but can over- or underestimate risk to humans because of species differences.⁸ Due to these difficulties, ~30% of new drug candidates fail due to toxicity issues that are not discovered until clinical testing.^{9,10}

Simple, fast, reliable, and inexpensive molecular-based in vitro methods for initial screening of compounds to complement cell-based bioassays are largely nonexistent. Realizing this fact, we recently developed inexpensive electro-optical arrays based on visible electrochemiluminescence (ECL) light emission to detect chemical reactions between metabolites and DNA. These arrays measure relative DNA damage rates from reactive metabolites generated by enzymes in ultrathin films.^{11–13} The arrays feature multiple spots constructed layer-by-layer (LbL) from metabolic enzymes, DNA,

and the ECL-emitting ruthenium(II)polyvinylpyridine polymer $[\text{Ru}(\text{bpy})_2\text{PVP}_{10}]^{2+}$ (RuPVP) on a 1×1 in. chip of conductive pyrolytic graphite (PG). The chip is a solid electrode with up to 50 spots differentiated by position and allows measurement of ECL with a charge coupled device (CCD) camera from an open-top electrochemical cell (Supporting Information, Scheme S1). In the measurement step, Ru^{II}PVP is electrochemically oxidized to Ru^{III}PVP, which reacts with DNA in a complex pathway to produce excited state $^*\text{Ru}^{\text{III}}\text{PVP}$ sites that decay to give ECL at 610 nm.¹⁴

Toxicity screening is achieved by first using the ECL arrays to enzymatically convert test chemicals into metabolites. Reactive metabolites are trapped in the spots by ds-DNA as covalent nucleobase adducts (Supporting Information, Scheme S1A). The second step is detection of DNA damage by applying voltage to the array and capturing the ECL image (Supporting Information, Scheme S1B). Integrated ECL intensity increases when DNA is damaged because of the partially disrupted DNA structure, facilitating faster oxidation of guanines by Ru^{III}PVP sites by shortening the average distance between them.¹⁴ The ds-DNA here is not protected by histones or other cell components, so the arrays predict only the possibility of DNA damage from reactive metabolites produced by the enzyme reactions.

Received: January 7, 2011

Accepted: February 26, 2011

Published: March 11, 2011

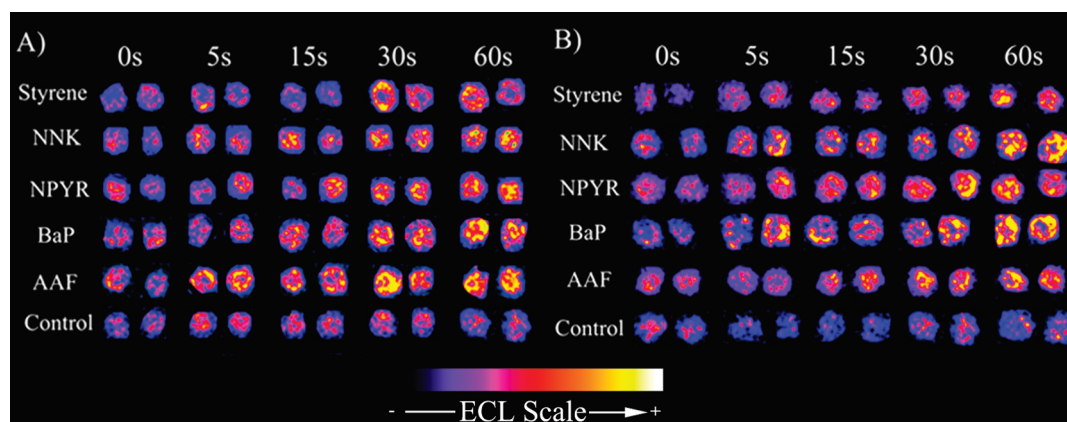


Figure 1. Reconstructed ECL array data for a series of enzyme reaction times using DNA/RuPVP/enzyme spots. Enzyme sources were human microsomes/cytosol (human liver enzymes, HLE) for (A) and rat liver microsomes/cytosol (rat liver enzymes, RLE) for (B). Concentrations of substrates: 0.2 mM styrene, 0.2 mM NNK, 0.2 mM NPYR, 0.05 mM BaP, and 0.025 mM 2-AAF using an NADPH regeneration system for denoted time in seconds. Controls were exposed to only NADPH.

Slopes of ECL increase vs enzyme reaction time using these arrays were proven to correspond to relative DNA damage rates by correlations with formation rates of major nucleobase adducts measured by liquid chromatography (LC)-MS using DNA/enzyme films on nanoparticles.^{11–13,15} Slopes of ECL increase vs reaction time also correlated with rodent liver TD₅₀, the chronic dose for inducing liver tumors, for a limited set of compounds.¹³ We also used these arrays to confirm species differences in ds-DNA damage rates by tamoxifen using enzymes from rat vs human liver.¹⁶

A universal ECL array genotoxicity platform would be a valuable addition to in vitro toxicity bioassays for early screening of commercial chemical candidates. To move toward this goal, we report here a representative array platform featuring a broad range of microsomal and cytosolic enzymes¹⁷ that facilitates detection of DNA-reactive species from nearly all common metabolic pathways. The array utilizes metabolic enzymes from rat and human liver microsomes and rat and human liver cytosol and includes mouse liver S9 fractions for the first time to represent human and rodent metabolism. We evaluate this new array by comparing 11 chemicals under identical conditions at optimal concentrations for signal development. Correlations of ECL array data to genotoxicity bioassay data and rodent toxicity metrics were evaluated for this group of compounds.

EXPERIMENTAL SECTION

Chemicals and Materials. Full experimental details and sources of chemicals are reported in the Supporting Information.

Array Fabrication. ECL arrays were made as previously described.^{12,13} Calf thymus ds-DNA, RuPVP, and enzyme were deposited by pipetting 0.5 μ L drops of solution on PG blocks. Final spot compositions represented as the order of layer deposition are DNA/(RuPVP/DNA)₂/RuPVP/DNA/human liver cytosol/RuPVP/DNA/human liver microsomes, DNA/(RuPVP/DNA)₂/RuPVP/DNA/rat liver cytosol/RuPVP/DNA/rat liver microsomes, and DNA/(RuPVP/DNA)₂/(RuPVP/DNA/Mouse S9)₂. For brevity, spots are generally denoted as DNA/RuPVP/enzyme, DNA/RuPVP/HLE, DNA/RuPVP/RLE, DNA/RuPVP/MLE, where HLE denotes human liver enzymes from liver microsomes/cytosol, RLE represents the corresponding rat liver enzymes, and MLE is mouse S9 liver fraction.

Reaction with DNA Damaging Agents. *Safety Note:* all test compounds are suspected human carcinogens. Procedures should be done wearing gloves in a closed hood. Incubations were done on arrays by spotting 50 μ L incubating solutions containing test chemical and enzyme cofactors onto four DNA/RuPVP/enzyme spots at 37 °C for up to 60 s. The array was rinsed rapidly with water to stop the reaction.

ECL Measurement. After enzyme reactions, the array was placed in an open top electrochemical cell filled with pH 5.5, 10 mM buffer + 0.15 M NaCl.¹² A potential of 1.25 V vs Ag/AgCl was applied to the array for 30 s to develop ECL which is acquired over this time by the CCD camera.

RESULTS

Film Characterization. Film compositions used in the array were characterized by making the films on 9 MHz quartz crystal microbalance (QCM) gold-quartz resonators. Frequency shifts after each layer were deposited, dried, and used to calculate the weight of each component and nominal film thickness (Supporting Information, Table S1).¹⁸ QCM frequency decreased linearly with increasing layer number, indicative of stable, reproducible film growth (Supporting Information, Figure S1). Films had about 40 nm thicknesses, suggesting that reactions will not be limited mass transport processes.¹⁹

Single-Enzyme Bioactivation. Test chemicals were *N*-acetyl-2-aminofluorene (2-AAF), *N*-nitrosopyrrolidine (NPYR), 4-(methylnitrosamino)-1-(3-pyridyl)-1-butanone (NNK), benzo[*a*]pyrene (BaP), and styrene. These compounds have well understood DNA-metabolite adduct formation via cytochrome P450 (cyt P450)-catalyzed oxidations. Figure 1 portrays reconstructed ECL images of a representative set of array spots containing (A) human liver microsomes/cytosol (HLE) and (B) rat liver microsomes/cytosol (RLE), exposed to low, medium, and high concentrations of substrates using an NADPH regenerating system to activate cyt P450s. Increased ECL intensity was observed after the DNA/RuPVP/enzyme film spots were exposed to different substrates suggesting DNA damage. As mentioned earlier, the rate of ECL increase versus enzyme reaction time in the ECL arrays reflects the relative rate of DNA damage.^{12,13,17} Control spots exposed to only an NADPH generating system showed negligible ECL increases (Figure 1). Control spots with enzymes incubated

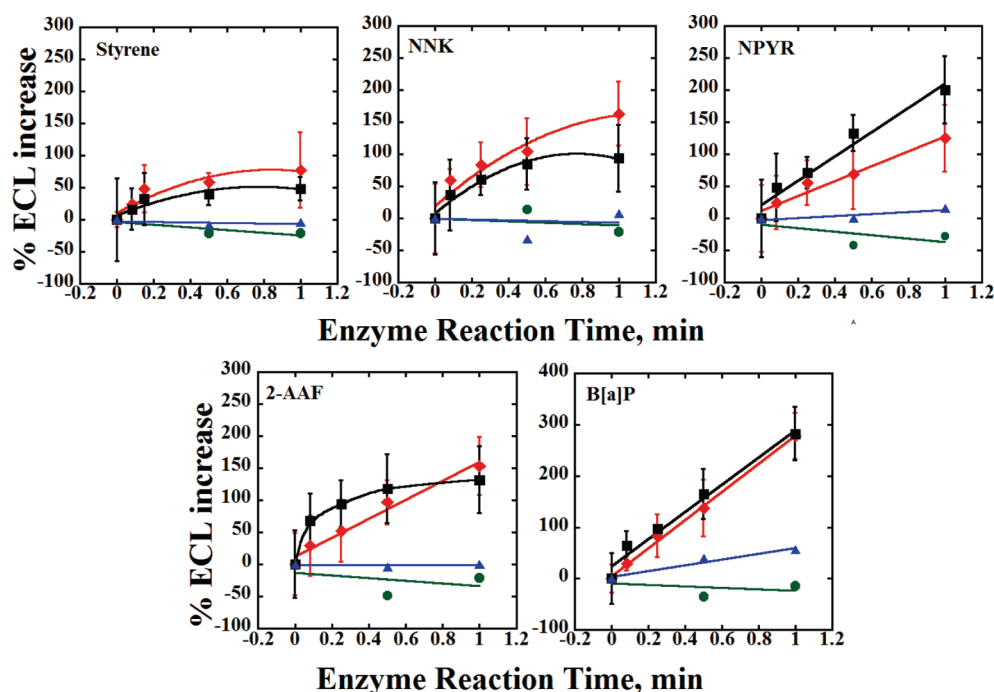


Figure 2. Influence of enzyme reaction time on enzyme mass-normalized ECL for arrays with RLE (red \blacklozenge) and HLE (\blacksquare) using the NADPH regenerating system for reaction with different substrates. Enzyme mass (μg) was estimated as $n \times 0.04$ (avg. spot area, cm^2) \times mean mass per unit area from QCM ($\mu\text{g cm}^{-2}$, Supporting Information, Table S1), where n is number of enzyme layers. Controls are incubations with substrates only for spots containing RLE (green \bullet) or HLE (blue \blacktriangle). Substrate concentration: styrene, NNK, and NPYR, 0.2 mM; 2-AAF, 0.025 mM; BaP, 0.05 mM.

with substrates, but no NADPH, did not generate ECL increases (not shown).

Relative ECL intensities normalized for enzyme mass in the spot are presented as %ECL increase vs enzyme reaction time (Figure 2). Error bars reflect ECL reproducibility within $\pm 8\%$ for 12 replicates on 3 or more arrays at each reaction time. ECL increases ranged from 70% to 300% for array spots for different substrates using HLE and RLE (red and black). Control spots exposed to only substrates produced negligible ECL changes (green and blue), suggesting no detectable DNA damage. Different ECL responses were found for reactions catalyzed by RLE and HLE for styrene, NNK, NPYR, and 2-AAF. There was no statistically significant difference for BaP when RLE or HLE was used (student t test, 95% confidence). These data were obtained after identifying the range of substrate concentrations giving readily measurable ECL increases for 1 min enzyme reactions. Slopes of normalized ECL increases for different concentrations were within $\pm 10\%$ when divided by substrate concentration. At 0.2 mM, NNK and NPYR produced about 2–3 times more ECL than styrene using either RLE or HLE (Figure 2), suggesting more DNA damage. A lower concentration (0.025–0.05 mM) was sufficient for 2-AAF and BaP to generate comparable ECL increases. 2-AAF gave a nonlinear ECL increase using HLE and a linear increase using RLE. BaP gave a similar linear ECL increase using both RLE and HLE (Figure 2). As discussed later, these observations led us to use the initial slopes of ECL vs reaction time estimated at zero reaction time and normalized for enzyme and substrate mass to compare array results with other toxicity indices.

Multienzyme Bioactivations. These experiments were done on 1-naphthylamine (1-NA), 2-naphthylamine (2-NA), 2,4-diaminotoluene (2,4-DAT), 2,6-diaminotoluene (2,6-DAT), 4-amino-biphenyl (4-ABP), and 2-aminofluorene (2-AF). These arylamines

are environmental contaminants derived from tobacco, industrial, and agricultural uses.^{20–22} Arylamines form reactive N -hydroxylated derivatives by cyt P450 oxidation.²³ Further conjugation of N -hydroxy arylamines by acetyl- or sulfo-transferases produces conjugates subject to acid hydrolysis to DNA-reactive nitrenium intermediates.²⁴

The arylamines were tested with an ECL array equipped for multistep enzyme bioactivation. HLE and MLE incorporated into array spots served as sources of cyt P450s and N -acetyltransferases (NATs). Reconstructed images (Supporting Information, Figure S2) show ECL response after enzyme reactions for HLE (A) and MLE (B) exposed to arylamines. AcCoA was included to activate NATs. Figure 3 shows array data expressed as enzyme-normalized ECL increase vs reaction time. In general, spots with HLE gave larger ECL increases than those with MLE for the same substrate incubation conditions (t test, 95% confidence). Slopes of %ECL increase vs reaction time ranked in decreasing order as follows: 4-ABP > 2-AF \geq 2, 4-DAT \geq 2-NA > 2, 6-DAT > 1-NA.

Correlation with Other Toxicity Metrics. Data for Comet and Ames assays and in vivo rodent toxicity are summarized in Table S2 (Supporting Information). To explore correlations with array data, initial slopes of ECL vs enzyme reaction time (k) (Figures 2 and 3) were further normalized by reactant concentration $[S]$ to define a fully normalized toxicity screening parameter, ECL turnover rate R :

$$R = k/[S] (\mu\text{g protein}^{-1} \cdot \text{min}^{-1} \cdot \text{mM}^{-1}) \quad (1)$$

(Supporting Information, Table S2). R -values were constant within $\pm 10\%$ at various values of $[S]$ giving measurable increases in ECL within 1 min enzyme reactions. Before discussing these correlations in detail, we present a brief overview of the related toxicity assays and what they measure.

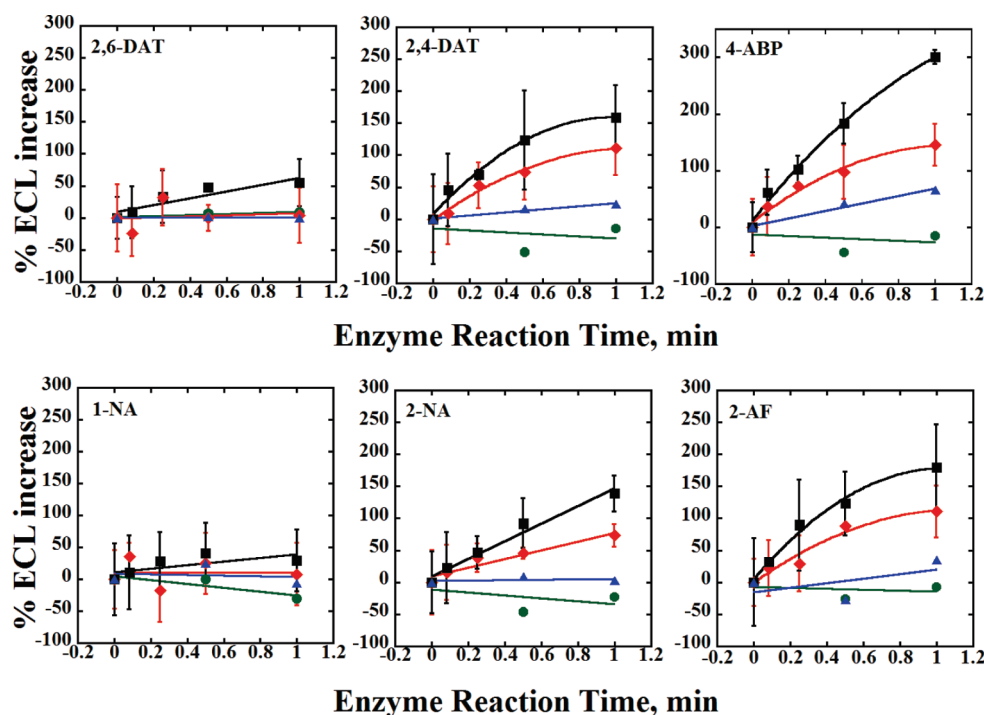


Figure 3. Influence of enzyme reaction time on enzyme mass-normalized ECL for spots with MLE (red \diamond), HLE (\blacksquare) with 0.2 mM arylamine substrates together with AcCoA and an NADPH regeneration system, and control incubation (green \bullet for MLE, blue \blacktriangle for HLE) with only 0.2 mM arylamines.

Ames *Salmonella* mutation tests are widely used to assess mutagenicity. The Ames test utilizes strains of *Salmonella typhimurium* containing a number of mutations in genes requiring histidine for growth.²⁵ Gene mutagens can induce reverse mutation of the bacteria yielding revertant colonies in the absence of histidine. The variable measured is the number of revertant colonies, also called revertants, taken to correspond to the mutagenic potential of the test chemical. Bacterial strains like TA1538 and TA1535 are specifically designed to detect respective frameshift (insertion or deletion of a nucleotide) and missense (change in one nucleotide) mutations.²⁶ Liver homogenates from rat or human are used as enzyme sources.²⁶

The Comet assay detects DNA damage caused by single or double strand breaks, base damage, and cross-links. Cell lines incubated with toxic chemicals generate broken DNA fragments which stream further from the nucleus during electrophoresis than intact DNA, creating a "tail". The product of tail length and fractional amount of DNA in the tail is defined as olive tail moment (OTM) and used as a measure of DNA damage.^{27,28} For consistency of metabolic enzyme sources, Comet assay data from human hepatic cell lines were chosen for comparison if available.

In vivo animal toxicity is represented by lethal dose (LD_{50}) and TD_{50} from rodents. Liver TD_{50} is the chronic dose (mg/kg body weight per day) inducing mixed liver tumors in half of a test male rodent population at the end of the standard life span.²⁹ LD_{50} is the lethal single dose in mg/kg body weight of a chemical that causes the death of 50% of the rodents and is a measure of acute toxicity.³⁰ The Berkeley Carcinogenic Potency³¹ and United States National Library of Medicine³² databases were the sources of rodent TD_{50} and LD_{50} values. Due to incomplete available data, values from rat species were employed for BaP, 2-AAF, NPYR, NNK, and styrene while mouse LD_{50} and liver TD_{50} (labeled with *) were used for arylamines. Obviously, a chemical with small LD_{50} and liver TD_{50} values is a very potent

poison, but TD_{50} measures chronic liver tumorigenicity and LD_{50} measures general acute toxicity.

Figure 4 shows correlations between normalized ECL turnover rates (R , eq 1) and Ames and Comet assay data. Figure 5 presents correlations of R with TD_{50} and LD_{50} . All R -values in these figures indicate a significant rate of DNA damage related to substrate metabolism. First, array results show slightly different ECL R -values for human liver enzymes and rodent liver enzymes for the same substrate. These variations may be related to species genotoxicity differences.¹⁶

Correlations of R with Ames data for BaP, 2-AAF, arylamine 2-NA, 2,4-DAT, and 4-ABP using TA 1538 strains (Figure 4A) were quite good. However, known tobacco carcinogens NNK and NPYR generated moderate R -values but are not mutagenic using Ames TA1538 strains and only slightly mutagenic using TA1535 (Supporting Information, Table S2). Similarly, 2-AF gives a moderate R -value and does not induce mutations using TA1535 but is highly mutagenic using TA1538.

Correlation of R with Comet assay data was good for most substrates (Figure 4B). Compounds with small OTM/conc. have low R including styrene, NNK, and NPYR, and those with large OTM/conc. have large R -values like 2-AAF and BaP.

Low LD_{50} or TD_{50} are indicative of high toxicity, so inverse LD_{50} or TD_{50} values ($1/LD_{50}$ or $1/TD_{50}$) were used in correlation graphs. TD_{50} and LD_{50} from mouse were used for arylamines to compare with activation by MLE in ECL arrays and are labeled with an asterisk (*) in Figure 5. Approximate correlations between R and $1/TD_{50}$ (Figure 5A) and between R and $1/LD_{50}$ (Figure 5B) were found, since in most cases, compounds with relatively large $1/TD_{50}$ or $1/LD_{50}$ values produced high R including 2-AAF and BaP whereas styrene, NPYR, and 2,4-DAT with small LD_{50} generated low ECL. Exceptions include 2-AF, 1-NA, and 2-NA that did not generate large R in arrays.

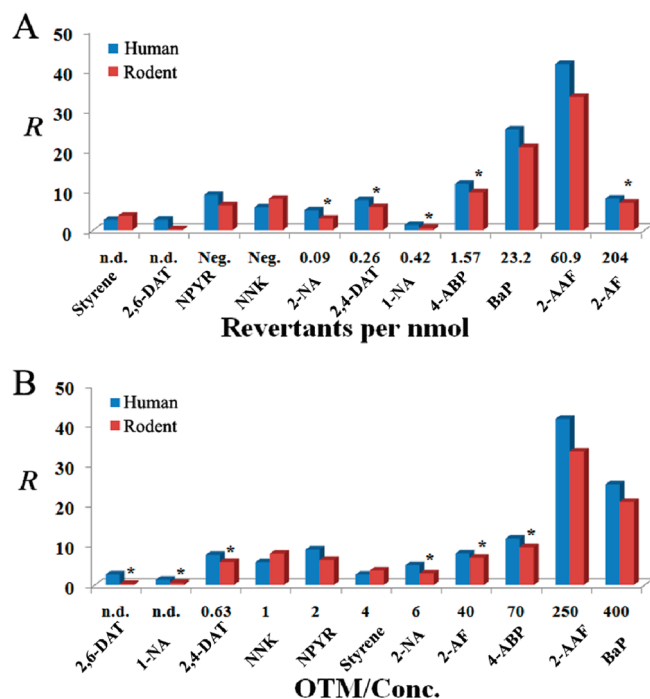


Figure 4. Correlation of normalized ECL turnover rate R ($\mu\text{g protein}^{-1} \cdot \text{min}^{-1} \cdot \text{mM}^{-1}$) with (A) the revertants per nmol from Ames tests, TA1538 strain, and (B) OTM/[S] values from Comet assays (see Supporting Information, Table S2). Asterisk (*) denotes OTM data from mouse; other values are for rats. Neg. = negative results, n.d. = not determined.

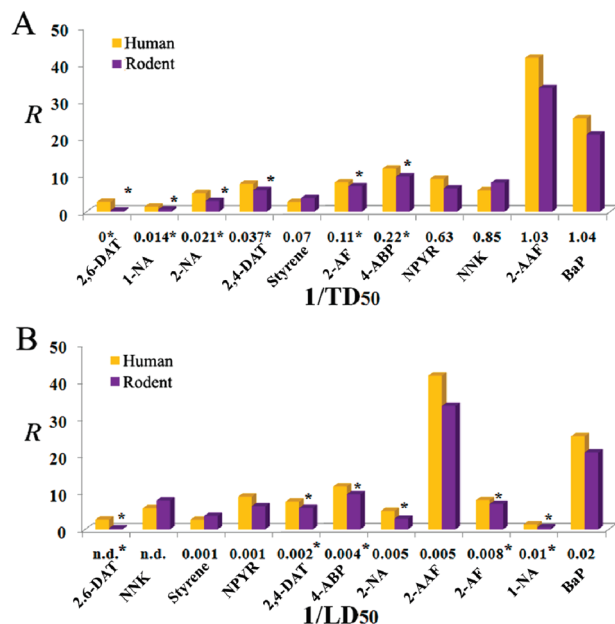


Figure 5. Correlation of normalized ECL array turnover rate R ($\mu\text{g protein}^{-1} \cdot \text{min}^{-1} \cdot \text{mM}^{-1}$) with (A) $1/\text{TD}_{50}$ and (B) $1/\text{LD}_{50}$ (see Supporting Information, Table S2). Asterisk (*) denotes data from mouse; other values are for rats. n.d. = not determined.

DISCUSSION

Results above demonstrate the value of ECL arrays featuring an expanded representative collection of metabolic oxidation and

bioconjugation enzymes for toxicity screening. As with previous versions of ECL arrays,^{12,13} relative DNA adduct formation rates are provided for potentially toxic metabolites as predictors of genotoxicity, as demonstrated here for a collection of chemicals. In vitro toxicity screening can be done without cell cultures, and results reflect the relative DNA damage rates by metabolites formed. The arrays are inexpensive, utilizing only an unprocessed carbon block, conventional electrochemical equipment, a CCD camera, and a dark box. Enzyme reaction steps can be completed in 1 min, and ECL signal development takes ~ 30 s, so that the toxicity screening of several compounds at different concentrations can be done rapidly compared to bioassays such as the Ames test and the Comet assay (usually 24 h or longer). Bioconjugation reactions can be turned on and off at will by including or omitting the relevant enzyme cofactors, providing a further diagnostic tool to assess the enzyme source of reactive metabolites. While QCM studies are required to establish amounts of protein deposited in the spots, these experiments need not be repeated for subsequent use of a given array featuring the same spots.

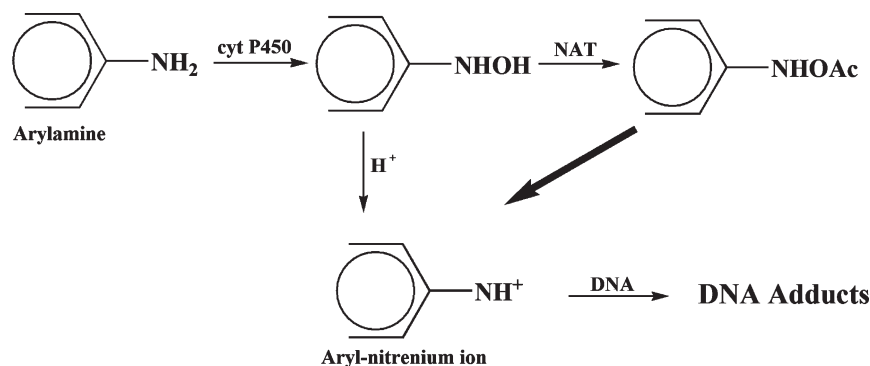
In this paper, we defined the slope of ECL increase vs enzyme reaction time normalized for amounts of enzymes and substrate concentration as a parameter R (eq 1) to facilitate comparisons of toxicity array data to that from conventional toxicity bioassays. Qualitatively reasonable correlations were obtained in most cases (Figures 4 and 5). Clearly, compounds such as styrene which have significant but relatively low toxicity by conventional bioassays give small R -values, and chemicals with relative high levels of toxicity in bioassays (e.g., 2-AAF and BaP) give large R -values. In addition, toluene has very high TD_{50} and LD_{50} (5390³¹ and 2250³²), and DNA adduct formation is not detected under our array conditions, providing a good negative control.

The variations in R -values when human and rodent liver enzymes are used (Figures 4 and 5) can be explained by species differences in amounts, identities, and activities of metabolic enzymes.^{33,34} Measured differences could serve as important tools to predict when toxic manifestations differ between humans and rodents. We have already demonstrated elucidation of such species differences with tamoxifen using an earlier version of ECL arrays.¹⁶

For compounds like styrene, NNK, NPYR, BaP, and 2-AAF, which involve DNA adduct formation from one-step cyt P450 bioactivation,^{35–37} results reflect different rates of DNA damage after enzyme activation. Regardless of rodent or human enzyme source, 2-AAF and BaP induced a large ECL increase at relatively low concentrations (25 or 50 μM) suggested that their metabolites are very reactive toward DNA. Styrene is much less DNA-reactive upon activation since a notable ECL increase can only be observed at a relatively high concentration (1 mM). This concentration effect is suitably accounted for by normalization in the R parameter.

Intermediate concentrations of NPYR and NNK (0.2 mM) were needed to produce measurable ECL increases, which are likely to be related to two factors. First, α -hydroxylation of NNK and NPYR by cyt P450 generates active diazonium ions which can hydrolyze in water; as a result, a higher substrate concentration is necessary to produce a detectable amount of reactive metabolite-DNA adduct(s) in aqueous media.^{36,38} Second, the bulky N^7 -guanine adduct(s) from BaP activation³⁹ may possibly contribute to a larger disruption of the DNA structure compared with the smaller N^7 -guanine adducts from NPYR and NNK.³⁶ Whether the latter factor can contribute significantly to the ECL signal is uncertain at this time.

Scheme 1. Major Metabolic Pathway of Arylamines Leading to DNA Adducts



The ability of the ECL array to differentiate relative DNA reactivity for metabolites of similarly structured compounds was demonstrated for arylamines. Scheme 1 summarizes the major pathway of arylamine metabolism, which involves bioactivation by cyt P450s to form *N*-hydroxy derivatives.²⁴ The second step is a conjugation whereby *N*-acetyltransferase (NAT) converts *N*-hydroxy intermediates into active esters using AcCoA.⁴⁰ Upon loss of $-\text{OAc}$, highly electrophilic arylnitrenium ions are formed that attack guanine bases. Also, *N*-hydroxy arylamines can yield arylnitrenium ions without the conjugation reaction. However, this process prefers a more acidic medium and may be slow under neutral conditions.²⁴

For arylamines, results with either HLE or MLE (Supporting Information, Table S2) showed $R_{1\text{-NA}} < R_{2,6\text{-DAT}} < R_{2\text{-NA}} < R_{2,4\text{-DAT}} < R_{2\text{-AF}} < R_{4\text{-ABP}}$ ($k_{1\text{-NA}} < k_{2,6\text{-DAT}} < k_{2\text{-NA}} < k_{2,4\text{-DAT}} < k_{2\text{-AF}} < k_{4\text{-ABP}}$). As the *N*-oxidation catalyzed by cyt P450s is an obligatory step for subsequent formation of $[\text{aryl-NH}^+]$, the initial slopes k in Figure 3 are associated with likelihood of oxidation at the arylamine nitrogens. Specifically, 1-NA undergoes preferred hydroxylation at the 2 position yielding 2-OH-1-NA whereas the major metabolite of 2-NA catalyzed by cyt P450s is *N*-OH-2-NA. Thus, a subsequent conjugation reaction for 1-NA (which is not *N*-hydroxylated) does not occur, limiting the formation of active intermediate. Specifically, the rate of *N*-oxidation of 2-NA was found to be >10-fold faster than that of 1-NA in a microsomal system, leading to ultimate reactive nitrenium formation,⁴¹ which partly explains the fast ECL turnover observed in Figure 3. 2-AF forms mainly *N*-hydroxy-2-AF, but its *N*-site is more electron-deficient than that in 2-NA; thus, 2-AF metabolite is more likely to be attacked by the active enzyme radicals giving $k_{2\text{-AF}} \approx 2k_{2\text{-NA}}$ (Supporting Information, Table S2). Array results were consistent with an earlier study in which the *N*-oxidation rate of 2-AF was about 3 times that of 2-NA using human liver cyt P450 1A2.⁴¹

Another isomer pair, 2,6-DAT and 2,4-DAT, both showed genotoxicity in the array, although 2,4-DAT had a 3-fold larger R than 2,6-DAT, correlated with a previous study on binding to DNA of these isomers using rat hepatocytes.⁴² 4-ABP induced the largest R , indicative of the most toxic compound. Again, similar results were obtained in studies on binding affinity of four arylamines to bladder epithelium DNA in which 4-ABP metabolites have the strongest reactivity to DNA followed by 2-AF, 2-NA, and 1-NA.⁴³

R -values correlated reasonably with in vitro and in vivo toxicity data (Figure 4 and 5), demonstrating the utility of ECL arrays to differentiate potential toxicity of compounds with or without similar structures and metabolic pathways. It should be realized,

however, that the bioassays compared to the ECL arrays are measuring different things; albeit, all are generally related to toxicity. Ames and Comet assays measure bacterial reverse mutation or DNA damage in cells. TD_{50} measures chronic rodent toxicity relative to carcinogenesis, and LD_{50} is a crude measure of acute toxicity. On the other hand, the ECL arrays measure the rate of chemical reaction of metabolites with DNA in a cell-free biochemical system. The R -values reflect rates of DNA damage under ideal, nonbiological conditions. We believe that the value of these methods, as well as additional ones, lies in their combined use in a panel for human toxicity prediction.

The rough correlations between R and the other toxicity metrics (Figures 4 and 5) need to be understood in the above context. For example, lower correlation of R and Ames data may reflect limitations of the bacteria model, metabolic differences between enzymes in the two tests, and relative and specific differences between Ames and ECL arrays. Comet assay data presented better correlation with R , perhaps because both assays have DNA damage end points. Rodent $1/\text{LD}_{50}$ were less related to R for arylamines yet fairly well correlated for styrene, NPYR, 2-AAF, and BaP. TD_{50} shows better correlation to ECL array data with rodent enzymes, as expected from similarity of activation by enzymes in the ECL arrays and the rodents themselves. Most importantly, as expected, mouse $1/\text{TD}_{50}$ correlated well with R using mouse liver enzymes for arylamines (Figure 5A). The reason that 2,6-DAT shows small but significant R values in ECL array but fails to induce liver tumors in rat models may be associated with faster detoxification in vivo.^{44–46}

In summary, we have presented and validated here a metabolically representative ECL array by testing 11 chemicals of varying toxicity and exploring correlations with rodent TD_{50} and LD_{50} , Ames tests, and Comet assays. Species differences between rodents and humans can be assessed using appropriate enzyme sources in the arrays. Results support the value of ECL genotoxicity arrays in early screening of unknown chemicals or drugs to assess the possibility of metabolite reactions with DNA. Coupled with existing toxicity bioassays, ECL arrays can provide metabolite reactivity data to complement the prediction of human toxicity.

■ ASSOCIATED CONTENT

S Supporting Information. Detailed experimental procedures and one scheme of experiment setup, a figure and a table describing quartz crystal microbalance characterization, a figure of addition ECL array images, and a table with toxicity metric

values. This material is available free of charge via the Internet at <http://pubs.acs.org>.

AUTHOR INFORMATION

Corresponding Author

*E-mail: james.rusling@uconn.edu.

ACKNOWLEDGMENT

This work was supported financially by US PHS grant No. ES03154 from the National Institute of Environmental Health Sciences (NIEHS), NIH, USA.

REFERENCES

- (1) Apruzzese, W. A.; Vouros, P. J. *Chromatogr., A* **1998**, *794*, 97–108.
- (2) Farmer, P. B.; Brown, K.; Tompkins, E.; Emms, V. L.; Jones, D. J. L.; Singh, R.; Phillips, D. H. *Toxicol. Appl. Pharmacol.* **2005**, *207*, 293–301.
- (3) Tarun, M.; Rusling, J. F. *Crit. Rev. Eukaryotic Gene Expression* **2005**, *15*, 295–316.
- (4) Kramer, J. A.; Sagartz, J. E.; Morris, D. L. *Nat. Rev. Drug Discovery* **2007**, *6*, 636–649.
- (5) Mayne, J. T.; Ku, W. W.; Kennedy, S. P. *Curr. Opin. Drug Discovery Dev.* **2006**, *9*, 75–83.
- (6) Boysen, G.; Hecht, S. S. *Mutat. Res.* **2003**, *543*, 17–30.
- (7) Isfort, R. J.; LeBoeuf, R. A. *Mutat. Res.* **1996**, *365*, 161–173.
- (8) Infante, P. F. *Environ. Health Perspect.* **1993**, *101* (Suppl 5), 143–148.
- (9) Caldwell, G. W.; Yan, Z. *Curr. Opin. Drug Discovery Dev.* **2006**, *9*, 47–60.
- (10) Nassar, A. E. F.; Kamel, A. M.; Clarimont, C. *Drug Discovery Today* **2004**, *9*, 1055–1064.
- (11) Rusling, J. F.; Hvastkovs, E. G.; Schenkman, J. B. In *Drug Metabolism Handbook*; Nassar, A., Hollenburg, P. F., Scatina, J., Eds.; J. Wiley, Hoboken, NJ, 2009, pp 307–340.
- (12) Hvastkovs, E. G.; So, M.; Krishnan, S.; Bajrami, B.; Tarun, M.; Jansson, I.; Schenkman, J. B.; Rusling, J. F. *Anal. Chem.* **2007**, *79*, 1897–1906.
- (13) Krishnan, S.; Hvastkovs, E. G.; Bajrami, B.; Choudhary, D.; Schenkman, J. B.; Rusling, J. F. *Anal. Chem.* **2008**, *80*, 5279–5285.
- (14) Dennany, L.; Forster, R. J.; Rusling, J. F. *J. Am. Chem. Soc.* **2003**, *125*, 5213–5218.
- (15) (a) Krishnan, S.; Hvastkovs, E. G.; Bajrami, B.; Schenkman, J. B.; Rusling, J. F. *Mol. Biosyst.* **2009**, *5*, 163–169. (b) Krishnan, S.; Hvastkovs, E. G.; Bajrami, B.; Jansson, I.; Schenkman, J. B.; Rusling, J. F. *Chem. Commun.* **2007**, 1713–1715.
- (16) Zhao, L.; Krishnan, S.; Zhang, Y.; Schenkman, J. B.; Rusling, J. F. *Chem. Res. Toxicol.* **2009**, *22*, 341–347.
- (17) Zhao, L.; Schenkman, J. B.; Rusling, J. F. *Chem. Commun.* **2009**, 5386–5388.
- (18) Lvov, Y. In *Protein Architecture: Interfacing Molecular Assemblies and Immobilization Biotechnology*; Lvov, Y., Möhwald, H., Eds.; Marcel Dekker: New York, 2000, pp 125–167.
- (19) Munge, B.; Estavillo, C.; Schenkman, J. B.; Rusling, J. F. *ChemBioChem* **2003**, *4*, 82–89.
- (20) Kim, D.; Guengerich, P. F. *Annu. Rev. Pharmacol. Toxicol.* **2005**, *45*, 27–49.
- (21) Zayas, B.; Stillwell, S. W.; Wishnok, J. S.; Trudel, L. J.; Skipper, P.; Yu, M. C.; Tannenbaum, S. R.; Wogan, G. N. *Carcinogenesis* **2007**, *28*, 342–349.
- (22) Neumann, H. G. *Crit. Rev. Toxicol.* **2007**, *37*, 211–236.
- (23) Beland, F. A.; Kadlubar, F. F. *Environ. Health Perspect.* **1985**, *62*, 19–30.
- (24) Kadlubar, F. F.; Miller, J. A.; Miller, E. C. *Cancer Res.* **1977**, *37*, 805–814.
- (25) Ames, B. N.; Durston, W. E.; Yamasaki, E.; Lee, F. D. *Proc. Natl. Acad. Sci. U.S.A.* **1973**, *70*, 2281–2285.
- (26) Ames, B. N.; McCann, J.; Yamasaki, E. *Mutat. Res.* **1975**, *33*, 27–28.
- (27) (a) Olive, P. L.; Banáth, J. P.; Durand, R. E. *Radiat. Res.* **1990**, *122*, 86–94. (b) Olive, P. L.; Banáth, J. P.; Durand, R. E. *J. Natl. Cancer Inst.* **1990**, *82*, 779–783.
- (28) Brendler-Schwaab, S.; Hartmann, A.; Pfuhrer, S.; Speit, G. *Mutagenesis* **2005**, *20*, 245–254.
- (29) Peto, R.; Pike, M. C.; Bernstein, L.; Gold, L. S.; Ames, B. N. *Environ. Health Perspect.* **1984**, *58*, 1–8.
- (30) Zbinden, G.; Flury-Roversi, M. *Arch. Toxicol.* **1981**, *47*, 77–99.
- (31) Gold, L. S. *The Carcinogenic Potency Database*; <http://potency.berkeley.edu>.
- (32) United States National Library of Medicine; <http://chem.sis.nlm.nih.gov/chemidplus>.
- (33) Stiborova, M.; Borek-Dohalska, L.; Aimova, D.; Kotrbava, V.; Kukackova, K.; Janouchova, K.; Rupertova, M.; Ryslava, H.; Hudecek, J.; Frei, E. *Gen. Physiol. Biophys.* **2006**, *25*, 245–261.
- (34) Monteith, D. K.; Gupta, R. C. *Cancer Lett.* **1992**, *62*, 87–93.
- (35) Schrenk, D.; Gant, T. W.; Michalke, A.; Orzechowski, A.; Silverman, J. A.; Battula, N.; Thorgerirsson, S. S. *Carcinogenesis* **1994**, *15*, 2541–2546.
- (36) Hecht, S. S. *Chem. Res. Toxicol.* **1998**, *11*, 559–603.
- (37) Arlt, V. M.; Stiborova, M.; Henderson, C. J.; Thiemann, M.; Frei, E.; Aimova, D.; Singh, R.; Gamboa da Costa, G.; Schmitz, O. J.; Farmer, P. B.; Wolf, C. R.; Phillips, D. H. *Carcinogenesis* **2008**, *29*, 656–665.
- (38) Wang, M.; McIntee, E. J.; Shi, Y.; Cheng, G.; Upadhyaya, P.; Villalta, P. W.; Hecht, S. S. *Chem. Res. Toxicol.* **2001**, *14*, 1435–1445.
- (39) Neilson, A. H., Ed. *PAHs and Related Compounds*; Springer: Berlin, 1998.
- (40) Badawi, A. F.; Hirvonen, A.; Bell, D. A.; Lang, N. P.; Kadlubar, F. F. *Cancer Res.* **1995**, *55*, 5230–5237.
- (41) Hammons, G. J.; Guengerich, F. P.; Weis, C. C.; Beland, F. A.; Kadlubar, F. F. *Cancer Res.* **1985**, *45*, 3578–3585.
- (42) Furlong, B. B.; Weaver, R. P.; Goldstein, J. A. *Carcinogenesis* **1987**, *8*, 247–251.
- (43) Beland, F. A.; Beranek, D. T.; Dooley, K. L.; Heflich, R. H.; Kadlubar, F. F. *Environ. Health Perspect.* **1983**, *49*, 125–134.
- (44) Cunningham, M. L.; Burka, L. T.; Matthews, H. B. *Drug Metab. Dispos.* **1989**, *17*, 612–617.
- (45) La, D. K.; Froines, J. R. *Arch. Toxicol.* **1994**, *69*, 8–13.
- (46) (a) Cunningham, M. L.; Matthews, H. B. *Mutat. Res.* **1990**, *242*, 101–110. (b) Taningher, M.; Peluso, M.; Parodi, S.; Ledda-Columbano, G. M.; Columbano, A. *Toxicology* **1995**, *99*, 1–10. (c) Cunningham, M. L.; Foley, J.; Maronpot, R. R.; Matthews, H. B. *Toxicol. Appl. Pharmacol.* **1991**, *107*, 562–567.